IEEE Open Journal of
Vehicular Technology

Received 30 June 2023; accepted 30 July 2023. Date of publication 7 August 2023;
date of current version 1 September 2023. The review of this article was coordinated by Editor Tianqi Mao.

Digital Object Identifier 10.1109/OJVT.2023.3302511

Joint Power and Tilt Control in Satellite Constellation for NGSO-GSO Interference Mitigation

MAHDIS JALALI [1] (Graduate Student Member, IEEE), FLOR ORTIZ [1] (Member, IEEE), EVA LAGUNAS [1] (Senior Member, IEEE), STEVEN KISSELEFF [1] (Senior Member, IEEE), LUIS EMILIANI [2] (Senior Member, IEEE), AND SYMEON CHATZINOTAS [1] (Fellow, IEEE)

[1]Interdisciplinary Centre for Security Reliability and Trust (SnT), University of Luxembourg, 4365 Esch-sur-Alzette, Luxembourg
[2]Société Européenne des Satellites (SES), 6815 Betzdorf, Luxembourg

CORRESPONDING AUTHOR: MAHDIS JALALI (e-mail: mahdis.jalali@uni.lu).

This work was supported by the Luxembourg National Research Fund (FNR) through Project MegaLEO under Grant C20/IS/14767486.

ABSTRACT The number of non-geostationary orbit (NGSO) satellite constellations is growing persistently. Accordingly, co-channel interference with geostationary orbit (GSO) networks will inevitably affect the operation of NGSO and GSO satellites in the years to come. Towards protecting the well-established GSO systems from the interference produced by the newly launched NGSO satellite constellations, the international telecommunication union (ITU) has established regulations and evaluation metrics for the aggregated emitted power flux-densities from NGSO systems. In conformity with these regulations, the NGSO operators should avoid disruptive emissions, which could lead to acute service interruptions. To reduce the downlink interference levels and alleviate harmful service disconnectivity of satellite constellations, we propose a joint power and tilt control strategy to maximize user demand satisfaction. Our proposed method ensures that the equivalent power flux-density (EPFD) from satellite constellation satisfies the ITU regulatory limits while the radio resource management for the user service is optimized via power control and tilting. Simulation results analyzing EPFD levels and geographical dependencies and the performance of optimized LEO transmissions are presented, showing the benefit of the proposed technique in terms of service continuity and spectrum coexistence.

INDEX TERMS GSO-NGSO satellite co-existence, interference management, equivalent power flux-density, satellite tilting, demand satisfaction.

I. INTRODUCTION

Owing to the remarkable characteristics of the low earth orbiting (LEO) satellite constellations, including low transmission latency, ubiquitous coverage, global service, and low launch costs, the space community has witnessed an increasing proliferation of private ventures targeting global space-based internet coverage [1], [2]. In addition, the satellite industry is evolving promptly and the cost gap between satellite telecommunication and terrestrial networks has decreased throughout recent years. Besides, the integration of satellite components into the terrestrial infrastructure of sixth-generation (6G) communication networks is envisioned as a key component to ensure ubiquitous service [3], [4]. Accordingly, satellites have been deployed faster with more flexibility, making it easier for non-geostationary orbit (NGSO) satellite constellations to grow their market. As a result, the number of satellites in orbit increases and they have to share finite spectrum resources. These frequency bands are also shared with the geostationary orbit (GSO) systems, thereby introducing the potential for interference. Additionally to that, satellite operators are planning to launch constellations of thousands of satellites. Examples of these massive systems are SpaceX's Starlink, OneWeb, and Amazon's Kuiper satellite constellations [5]. Once these mega-constellations begin services, more satellites will utilize the same frequency bands, more geographical regions are covered, and more satellite footprints' will overlap, thus the probability of interference will rise drastically. This would potentially impact the incumbent GSO services and expose them to risks of notable co-channel interferences and radio communication service interruptions [6]. The international telecommunication union (ITU) regulates the utilization of the spectrum and defines limits for acceptable interference in Article 22 of [7]. NGSO systems should comply with these regulations to avoid unacceptable interference to GSO networks in the fixed-satellite and broadcasting-satellite services. Correspondingly, the densely populated orbits with constellations and the resulting co-channel interference emissions toward GSO systems necessitate interference management and mitigation [8]. The study in [9] emphasizes the employment of mitigation techniques and the probability of the in-line events for LEO to GSO interference. To address this challenge, different interference avoidance solutions have been introduced in the literature.

One common spatial interference avoidance method is the exclusion zone or arc avoidance technique. A co-existence scenario of GSO and NGSO systems employing arc avoidance is evaluated in [10]. In that study, the minimization of exclusion angle and bandwidth for a LEO satellite is assessed. The optimization problem considers the interference towards the GSO receiver by an equivalent power flux-density (EPFD) constraint and solves this with a genetic algorithm. Reference [11] compares the arc avoidance technique with band-splitting and look-aside methods for interference mitigation. The efficacy of these techniques is evaluated in terms of throughput degradation at the GSO ground station without studying the resulting EPFD. In particular, the exclusion zone method has been analyzed in our previous work on interference avoidance for GSO receivers [12]. The study concluded that, while useful in managing the interference levels for the ground stations, exclusion zones negatively impact service continuity which is impractical from the perspective of NGSO service providers. Thus, more dynamic solutions should be applied to comply with the regulatory framework in the radio regulations and ensure connectivity at the same time.

Furthermore, optimizing LEO satellite resources such as transmit power, bandwidth and etc. has been considered while coping with the co-channel interference of NGSO and GSO systems in the literature. In [13], authors have considered power optimization for the co-existence of multibeam LEO satellites with the GSO system. The service fairness for LEO users is maximized with the constraint on co-frequency interference evaluated by the signal-to-noise and interference ratio (SINR) received at the GSO earth station. The GSO satellite power is optimized as well as the LEO satellite transmission power to satisfy the required SINR threshold for the GSO system. A key consideration is that the adaptable GSO satellite transmission power assumption and the SINR constraint do not represent an applicable downlink interference evaluation for the GSO system protection. This is given to the fact that NGSO interference avoidance techniques should not cause modifications to the already existing GSO networks. Moreover, alongside, optimizing the satellite's transmit power, another mitigation technique is considered as cognitive radio. The cognitive radio technique enables spectrum sharing and optimizes bandwidth allocation and has been studied as an alternative solution in the GSO-NGSO co-existence. Authors in [14] investigate rate splitting multiple access in cognitive radio to maximize the sum rate of the LEO system. The power and the subcarrier beam allocation are optimized subject to the temperature limit of the GSO users. Another research on cognitive satellite networks is conducted in [15] that considers GSO-NGSO co-existence where the LEO satellite is the primary user and GSO is the secondary. This assumption of GSO systems as non-primary users is in contrast with ITU regulations except for the frequency band 18.8-19.3 GHz, where there are no specified EPFD limits [7].

Additionally, in order to avoid interference, The OneWeb first-generation constellation adopts a pitch strategy [16]. This technique is the same as the tilt method and reduces the inline interference events at lower latitudes. Reference [17] evaluates this progressive pitch method along with switching off beams, for a single orbital plane of multibeam LEO satellites. The number of turned-off beams and pitch angle values are optimized for the satellite. This is done through geometrical analysis to ensure the interference at the GSO receiver is less than 6% of the system noise. Their results have demonstrated the avoidance of harmful interference at the cost of shutting off partial beams. This pitch-based solution is also analyzed by [18] from the perspective of average capacity maximization constrained by the connectivity and interference limit. The authors have used a genetic algorithm to optimize the pitch angle and the number of turned-off beams. In this article, we have also considered the tilting strategy to explore the potential of this method in reducing interference.

According to the review above, most of the existing work on GSO-NGSO co-existence has assumed one single NGSO satellite as a source of interference. On the other hand, as defined by Article 22 of international telecommunication union (ITU) regulations [7], the aggregated emission power flux-density from all the co-frequency space stations of an NGSO constellation should not exceed the specified limits. Thus, for an accurate evaluation of the interference to GSO systems, the whole constellation of NGSO satellites should be considered. In this work, we consider a constellation of LEO satellites and assess the co-frequency interference. Unlike the existing works focusing on the signal quality for the GSO receiver, we apply the EPFD metric defined for the interference evaluation to consider ITU regulations and NGSO compliance with them. To the best of our knowledge, this is the first time the EPFD metric is used as a constraint for the radio resource optimization of the entire LEO constellation.

Furthermore, no prior study has exploited the joint optimization of power and tilt parameters for NGSO satellite constellations whilst considering EPFD level constraints. This approach offers a flexible and adaptable solution that can be customized for different satellite systems, regardless of their constellation configuration. In this article, we propose a methodology for interference mitigation with the objective of maximizing the demand matching capability in a LEO satellite mega constellation adopting joint power allocation and satellite tilt. Satellite tilting, in contrast to the beamforming technique which requires expensive equipment, is a readily available alternative that can be implemented using reaction wheels or other mechanisms. This approach allows satellite operators to efficiently manage interference while maximizing demand matching capabilities, without incurring the high costs and processing complexities associated with beamforming. Nonetheless, user demand satisfaction becomes a critical element when introducing satellite tilting, as the tilt may result in gaps in the coverage areas where customers are deployed. Our proposed algorithm factors in both the location of the users and their demands, and subsequently determines the optimal tilt angle for a minimized number of satellites.

Our main contributions can be summarized as follows:

- We provide an in-depth evaluation of downlink interference from a typical LEO mega constellation to GSO ground stations in terms of the EPFD metric. Different scenarios based on GSO receiver positions, LEO satellite transmit antenna, and power characteristics are assessed to impart a thorough analysis of interference through EPFD, defining worst-case scenarios and severe events of regulation violation. This first step helps us understand the need for mitigation techniques, which motivate the next contributions of our work.
- Aiming to comply with interference regulations, we propose a joint power and tilt optimization to maximize demand satisfaction for the LEO satellite constellation subject to aggregate EPFD constraints. A demand-aware design is proposed to save transmit power whenever possible while complying with the spectrum coexistence constraints imposed by ITU regulations. The formulated joint optimization problem is non-convex and difficult to solve efficiently.
- A novel approach to the non-convex joint power and tilt angle control optimization problem is proposed based on the knowledge acquired from EPFD analyses. Notably, We have successfully minimized the need for tilting to a minimized number of critical satellites, resulting in reduced operational difficulties.

The rest of this article is structured as follows. The simulation model and interference events and regulations are described in Section II. The joint power and tilt optimization problem is investigated in Section III-A. In Section III-B our proposed solution is introduced. We present interference evaluations for different scenarios and the simulation results for our proposed interference mitigation solution in Section IV. Finally, we conclude the article in Section V.

II. SYSTEM MODEL

We consider LEO and GSO satellites operating in Ka band and analyze the downlink co-frequency interference from the LEO satellite to the GSO earth station as illustrated in Fig. 1. For the sake of clarity, we adopt a popular NGSO constellation configuration similar to the one employed by OneWeb [16], which is a Walker-star constellation. It should be noted that our proposed methodology is not limited to this specific satellite constellation configuration and can be applied to a wide range of potential constellations. We assume one single beam providing coverage to the overall satellite field of view (FoV).[1] The single beam NGSO satellites serve the users in time slots by the time division multiple access (TDMA) method. We assume a single GSO satellite and ground station and denote the set and index of LEO satellites and their users with $i \in \{1, 2, 3, .., N\}$ and $u \in \{1, 2, 3, .., U\}$, respectively. It is important to acknowledge that in our analysis, we considered a worst-case scenario for the interference between GSO and NGSO satellites, where the GSO receiver is situated on the equator [19]. This scenario represents the most severe interference level among all possible inline events. By evaluating our proposed solution under these extreme conditions, we can ensure its effectiveness for less severe interference scenarios. This approach allows us to establish a robust solution that can effectively address a wide range of potential interference scenarios between GSO and NGSO satellite systems.

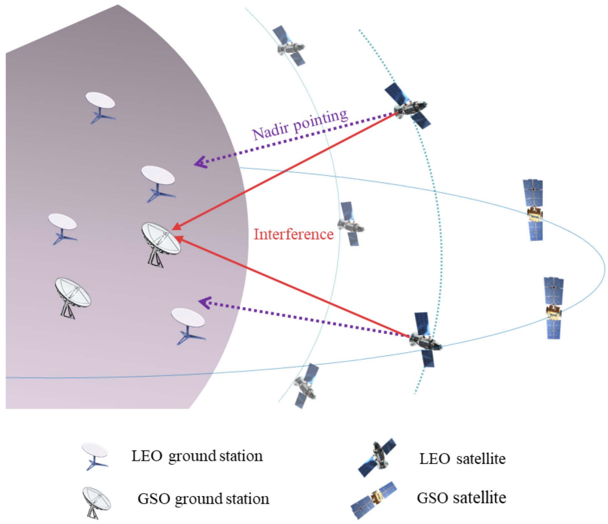

FIGURE 1. Co-existence of GSO and LEO satellites and interference events.

A. RECEIVED SIGNAL MODEL

1) SIGNAL RECEIVED AT GSO GROUND STATION

The received signals from NGSO satellites at the GSO ground stations are the interfering signals. Here, the interference calculations are carried out as described by ITU regulations [19]. The power flux-density radiated by a single NGSO satellite at any point of the earth is calculated as follows,

$$pfd = \frac{EIRP}{4\pi d^2}, \tag{1}$$

[1] While recent developments in LEO antenna architectures consider complex beamforming capabilities to generate narrower beams, our design is aimed at a general single beam LEO satellite. Such mono-beam can be seen as the coverage area of a beamforming-equipped LEO satellite.

where $EIRP$ is the equivalent isotropic radiated power of the NGSO satellite and d is the distance between the NGSO satellite and the receiving point on the earth's surface. With the definition of the power flux-density we define the EPFD metric which evaluates the aggregated emitted powers from interfering systems toward the victim. Depending on whether the interfering system is the satellite or the earth station, the EPFD-down and EPFD-up would be considered. As our focus in this study is the downlink interference, we consider the EPFD-down formulation to derive the EPFD at the GSO ground station as,

$$EPFD = 10\log_{10}\left(\sum_{i=1}^{N}\frac{P_i}{BW_{\text{ref}}}\frac{G^t\left(\phi_i^t\right)}{4\pi d_i^2}\frac{G_G^r\left(\phi_i^r\right)}{G_{Gmax}^r}\right), \quad (2)$$

where N represents the number of co-frequency satellites visible from the ground station, P_i is the transmitting power of the i-th satellite, BW_{ref} is the reference bandwidth, d_i is the distance between the NGSO satellite and the receiving station, $G^t(.)$ is the satellite transmit antenna gain in the direction of the GSO station denoted by angle ϕ_i^t, $G_G^r(.)$ is the receive GSO ground station antenna gain in the direction of NGSO satellite denoted by angle ϕ_i^r, and G_{Gmax}^r is the maximum antenna gain of the ground station antenna.

2) SIGNAL RECEIVED AT LEO USER

Now we present the received signal at the LEO user side. Concerning the channel model between i-th satellite and u-th user, $|h_{i,u}|^2$, we consider the model below [13],

$$|h_{i,u}|^2 = \frac{G^t\left(\varphi_{i,u}^t\right)G^r\left(\varphi_{i,u}^r\right)}{\left(4\pi r_{i,u}/\lambda\right)^2 L_{i,u}^{sh}L_{i,u}^{atm}}, \quad (3)$$

where $r_{i,u}$ is the distance between the satellite and user and λ indicates the wavelength. The satellite off-boresight transmit angle to the user is presented by $\varphi_{i,u}^t$, while the user antenna receive angle is presented by $\varphi_{i,u}^r$. $L_{i,u}^{sh}$ and $L_{i,u}^{atm}$ denote the shadowing loss and the atmospheric gas loss, respectively. The shadow fading is modeled by the log-normal formulation with the standard deviation values provided in [20]. In our simulations, the suburban scenario is considered and the shadowing loss is calculated by the standard deviation based on the elevation angle. The model in [21] is assumed for the atmospheric gas loss.

The interference at the LEO user is considered to be from the co-existing GSO satellite and the interference from neighboring NGSO satellites. The overall interference received at the u-th user served by the i-th LEO satellite is presented as follows,

$$I_{i,u} = \underbrace{\sum_{j\neq i} P_j|h_{j,u}|^2}_{\text{other LEO interference}} + \underbrace{P_G|h_{g,u}|^2}_{\text{GSO interference}}, \quad (4)$$

where g index refers to the GSO satellite and $|h_{g,u}|^2 = \frac{G_G^t(\varphi_{g,u}^t)G_G^r(\varphi_{g,u}^r)}{(4\pi r_{g,u}/\lambda)^2 L_{g,u}^{sh}L_{g,u}^{atm}}$ is the channel gain of the GSO satellite to the user. P_G, G_G^t, and G_G^r are the GSO satellite transmission power and antenna gain, and the GSO ground station receiver antenna gain, respectively. $r_{g,u}$ is the distance between the GSO satellite and LEO user. $\varphi_{g,u}^r$ and $\varphi_{g,u}^t$ represent the user receive antenna angle and the GSO satellite transmitting antenna angle, respectively. The SINR at the LEO user is as follows,

$$\text{SINR}_{i,u} = \frac{P_i|h_{i,u}|^2}{I_{i,u}+N_0B}, \quad (5)$$

where N_0 is the power spectral density of noise. The LEO intra-system interference term in (4) is typically minimized by implementing adequate frequency reuse schemes. For instance, the 4-color scheme, where the total bandwidth is split into two orthogonal blocks and combined with two orthogonal polarizations (hence the 4 colors) to ensure that no adjacent satellites operate on the same 'color'.

The capacity for a specific user of the i-th satellite is determined according to Shannon's capacity equation as follows,

$$C_{i,u} = B\log_2\left(1+\text{SINR}_{i,u}\right), \quad (6)$$

where B represents the LEO satellite bandwidth and $\text{SINR}_{i,u}$, the signal to interference plus noise ratio at the u-th user side of the i-th satellite. Assuming that each user has a traffic demand denoted by D_u, the LEO satellite system shall ensure that $C_{i,u}$ is matching the D_u demand.

B. BEAM PATTERN MODELS

The radiation pattern of the LEO satellite antenna is modeled according to [22]. The gain values, $G^t(.)$ in dBi unit can be computed from the formulation below:

$$G^t(\psi) = \begin{cases} G_{\max}^t - 3\left(\psi/\psi_b\right)^\alpha, & \psi_b \le \psi \le a\psi_b \\ G_{\max}^t + L_N + 20\log z, & a\psi_b < \psi \le 0.5b\psi_b \\ G_{\max}^t + L_N, & 0.5b\psi_b < \psi \le b\psi_b \\ X - 25\log\psi, & b\psi_b < \psi \le Y \\ L_F, & Y < \psi \le 90^\circ \\ L_B, & 90^\circ < \psi \le 180^\circ \end{cases}, \quad (7)$$

where

$$\begin{aligned} G_{\max}^t &= 20\log\left(\frac{D}{\lambda}\right) + 7.7 \\ X &= G_{\max}^t + L_N + 25\log\left(b\psi_b\right) \\ Y &= b\psi_b 10^{0.04(G_{\max}^t + L_N - L_F)} \\ L_B &= max\left(0,\, 15 + L_N + 0.25\,G_{\max}^t + 5\log z\right). \end{aligned} \quad (8)$$

$G_{\max}^t$ is the maximum gain of the antenna in the main lobe and depends on the antenna diameter D, and carrier frequency f. The wavelength is $\lambda = c/f$ and c denotes the light speed. ψ represents the angle from the main beam direction in degrees, and ψ_b is the one-half of 3 dB beamwidth. The values for L_N, L_f, z, α, a, and b are considered as -15 dB, 0 dBi, 1, 1.5, 2.58, and 6.32 respectively. For the configuration of GSO satellite antennas, we consider the beam pattern model in [23] which has the same formulation as (7) while the values for L_N, L_f,

z, α, a, and b are different, i.e. -20 dB, 0 dBi, 1, 2, 2.58, and 6.32 respectively.

The antenna pattern of the ground station receivers for both GSO and LEO are considered based on the reference radiation pattern for earth stations defined in [24]. We consider the following receive gain pattern $G^r(.)$, in dBi as,

$$G^r(\psi) = \begin{cases} G^r_{\max} - 0.0025\left(\psi \frac{D}{\lambda}\right)^2, & 0 \leq \psi \leq \psi_m \\ G_1, & \psi_m < \psi \leq 95\frac{\lambda}{D} \\ 29 - 25\log\psi, & 95\frac{\lambda}{D} < \psi \leq 33.1^\circ \\ -9, & 33.1^\circ < \psi \leq 80^\circ \\ -4, & 80^\circ < \psi \leq 120^\circ \\ -9, & 120^\circ < \psi \leq 180^\circ \end{cases}, \quad (9)$$

where

$$G^r_{\max} = 20\log\left(\frac{D}{\lambda}\right) + 7.7$$

$$G_1 = 29 - 25\log\left(\frac{95\lambda}{D}\right)$$

$$\psi_m = \left(\frac{20\lambda}{D}\right)\sqrt{G^r_{\max} - G_1}. \quad (10)$$

C. POWER CONTROL AND TILTING STRATEGY

In the scenario of the co-existence of GSO and NGSO systems, transmission power control on NGSO satellites represents a promising approach to prevent probabilities of interference. In some cases, however, the harmful emissions and the resulting EPFD can still be very significant, such that the transmit power of the LEO satellite may need to be substantially reduced compared to the usual transmit power level that is required to satisfy the demand. Although, reducing the power or turning off the satellite may not be a viable option for NGSO operators, as it could result in a waste of resources and degraded overall network performance. The tilting of the LEO satellite provides an additional degree of freedom that would help to reduce the EPFD at the GSO earth station while allowing higher transmit powers and thus signal quality at the intended receivers of the LEO satellite. Hence, we propose to combine the tilting method along with transmit power adaptation for LEO satellites to mitigate inline interferences. Specifically, we focus on the tilting direction in the north-south plane. This is better visualized by Fig. 2 where the satellite is tilted towards the North Pole. The LEO satellites are assumed to be nadir-pointing and when the tilting is applied the off-boresight angle of the antenna is changed. Depending on the location of the ground stations the tilting could result in an increase or decrease in the received power. As the goal of tilting is to alleviate interference with GSO receivers, its direction would be determined to point further away from the GSO ground station. Consequently, the off-boresight angle of LEO satellite antenna would increase, reducing the received gain and interfering effect. The resulting off-boresight angle of the NGSO satellite after tilting is calculated as,

$$\varphi^t_{tilt} = \varphi^t \pm \theta_{tilt}, \quad (11)$$

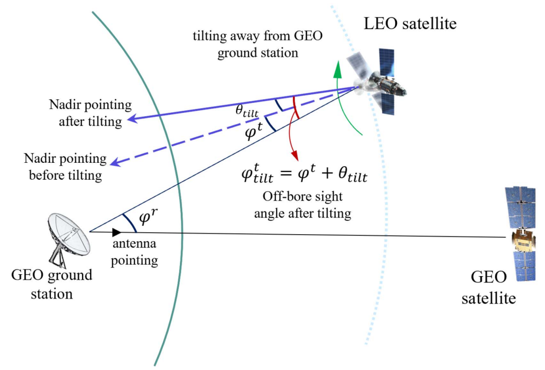

FIGURE 2. LEO satellite tilt strategy.

where φ^t_{tilt} is the off-boresight angle of the NGSO satellite to the ground station receiver and θ_{tilt} is the tilting angle (see Fig. 2 for illustration of the φ^t angle). The sign of the tilting angle will be determined by its direction and the regrading reference point on the ground. For instance, at the GSO ground station, the sign would be positive since the purpose of tilting is to point away from the GSO ground station and result in lower transmission antenna gain from the LEO satellite.

III. JOINT POWER ALLOCATION AND TILTING

In this section, we formulate the optimization problem. Our goal is to satisfy the demand of the LEO satellite users while taking into account the maximum tolerated EPFD generated at the GSO ground station.

A. PROBLEM FORMULATION

We optimize the transmission power of each LEO satellite and its tilting angle to minimize the Euclidean distance between traffic demand in the coverage areas of all satellites and the corresponding offered capacity:

$$\begin{aligned} \underset{P_i,\theta_i}{\text{minimize}} \quad & \left\| \left(C_{i,u} - D_u\right) \right\|_2 \\ \text{s.t.} \quad & L1: \text{EPFD} \leq \text{EPFD}_{\text{thr}}, \\ & L2: P_i \leq P_{\max}, \quad \forall i \\ & L3: 0 \leq \theta_i \leq \theta_{\max}, \quad \forall i, \end{aligned} \quad (12)$$

where $\|.\|_2$ denotes the ℓ_2-norm, D_u denotes the users' demand for each satellite, $L1$ is the interference limitation constraint, $L2$ represents the maximum power allocated by the LEO satellites, and $L3$ is the constraint on the maximum tilting angle of LEO satellites. The objective function minimizes the aggregated demand-capacity mismatch over all users of the visible LEO satellite set. It should be noted that our formulation is for a specific instance in time, and the optimization has to be repeated with some periodicity given the fact of LEO satellites' movement.

B. PROPOSED SOLUTION

We continue discussing the formulated problem by fitting a linear approximation for the satellite transmit antenna pattern in the (7) to avoid nonlinearity in our optimization problem. The transmission gain is fitted with an exponential formulation as,

$$G^t\left(\varphi^t\right) = A\exp\left(\beta\varphi^t\right), \tag{13}$$

where φ^t is the off-boresight angle of the NGSO satellite to the ground station receiver. By inserting the fitted antenna pattern in the interference constraint, $L1$, we obtain:

$$\tilde{L1} : 10\log_{10}\left(\sum_{i=1}^{N}\frac{P_iA\exp\left(\beta(\phi_i^t+\theta_i)\right)G_G^r(\phi_i^r)}{\mathrm{BW}_{ref}\,4\pi d_i^2\,G_{Gmax}^r}\right) \leq \mathrm{EPFD_{thr}}\,. \tag{14}$$

The nonlinearity of both the constraint $\tilde{L1}$ and the objective function is evident from the presence of the product of variable P_i and the exponential function of the LEO satellite's tilting angle in the above equation. This nonlinearity makes the problem formulated in (12) non-convex and challenging to solve efficiently.

We replace P_i by $exp(q_i)$, hence, the nonlinear product term transfers into the exponential of a linear function of the q_i and θ_i variables. The resulting capacity, $C_{i,u}$, in the objective function becomes:

$$B\log_2\left(1+\frac{k_{i,u}\exp\left(q_i+\beta s_{i,u}\theta_i\right)}{\sum_{j\neq i}k_{j,u}\exp\left(q_j+\beta s_{i,u}\theta_j\right)+v_u}\right), \tag{15}$$

with,

$$k_{i,u} = AG^r\left(\varphi_{i,u}^r\right)\exp\left(\beta\varphi_{i,u}^t\right)\lambda^2/(4\pi r_{i,u})^2$$
$$v_u = P_G|h_{g,u}|^2 + N_0B,$$

where $s_{i,u}$ denotes the sign of the tilting angle regarding the user direction, determining whether the tilting will increase or decrease the off-boresight angle, by taking values of ± 1.

The problem at hand can be simplified through the assumption of zero interference among LEO satellites. The LEO constellation would be designed to avoid self-interference by using different polarization for instance, and as a result, the emissions received from the neighboring satellite at the LEO user could be neglected [8]. In addition, based on our north-south tilting direction, when tilting a satellite, only one neighboring satellite may be affected, and even when considering the maximum tilt angle, the resulting interference is kept negligible (this is shown later in Fig. 4). The corresponding optimization problem is then derived as

$$\begin{aligned}
\underset{q_i,\theta_i}{\text{minimize}}\ & \left\|B\log_2\left(1+\frac{k_{i,u}\exp\left(q_i+\beta s_{i,u}\theta_i\right)}{v_u}\right)-D_u\right\|_2 \\
\text{s.t. } & \tilde{L1} : 10\log_{10}\left(\sum_{i=1}^{N}\frac{AG_G^r(\phi_i^r)\exp\left(q_i+\beta(\phi_i^t+\theta_i)\right)}{\mathrm{BW}_{ref}\,4\pi d_i^2\,G_{Gmax}^r}\right) \\
& \qquad \leq \mathrm{EPFD_{thr}}, \\
& L2 : q_i \leq \log(P_{\max}), \quad \forall i \\
& L3 : 0 \leq \theta_i \leq \theta_{\max}, \quad \forall i.
\end{aligned} \tag{16}$$

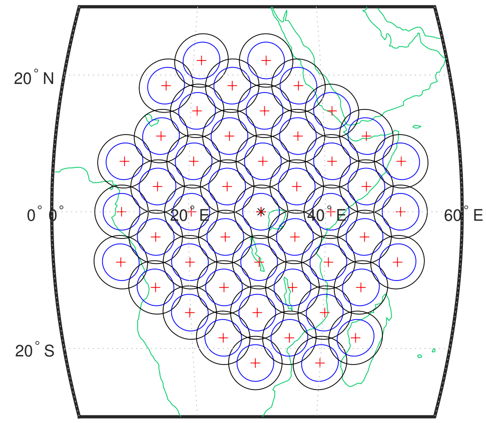

FIGURE 3. Visible LEO satellites and their −3 and −5 dB beam contours in blue and black, respectively.

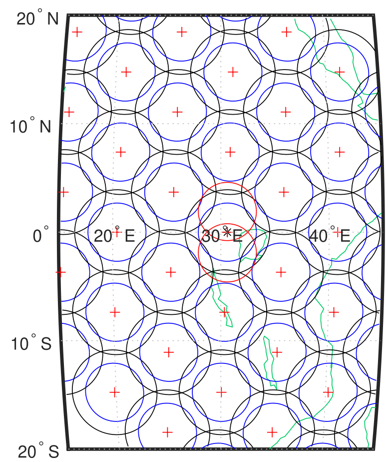

FIGURE 4. Maximum tilt angle for critical satellite and its resulting −3 dB beam contours for up or down tilt direction in red.

We can consider the objective function as a vector composition of functions, thus if the function inside the ℓ_2-norm is convex then the objective is convex [25]. To assess the convexity we apply a slack variable as $x_i = q_i + \beta s_{i,u}\theta_i$ in the function and have the resulting equation, $B\log_2(1 + (k_{i,u}/v_u)\exp(x_i)) - D_u$. This is convex due to the nonnegativity of its second derivative, noting that $k_{i,u}$ and v_u are positive by definition. Accordingly, the objective function of the problem is convex. Furthermore, the convexity of the $\tilde{L1}$ constraint can be verified by considering its log-sum-exp type [25]. Consequently, we can conclude that the optimization problem (16) is convex and can be solved by standard convex optimization methods.

Since tilting the whole visible satellites may not be cost-effective for the NGSO operators, one may prefer first to try to address the EPFD limitation from the power-control perspective and perform the tilting only to the satellites with high contribution to the aggregated interference. Following this intuition, we next propose an alternative to (16) where the goal is to minimize the number of satellites that perform tilting.

C. HEURISTIC SOLUTION FOR TILTING MINIMIZATION

In Section IV-A we conduct an evaluation of the EPFD results and conclude that the primary radiations leading to high EPFD results are emitted by the LEO satellites closest to the GSO receiver. These critical satellites, as we refer to them, serve as a key factor in our approach to reducing the complexity and costs associated with tilting multiple satellites. Therefore, we apply the tilting strategy exclusively to satellites which are critical in terms of interference.

For our proposed solution, first, we evaluate the contribution of each satellite to the EPFD limit by calculating a $\boldsymbol{\gamma}$ vector as

$$\gamma_i = \frac{AG_G^r\left(\phi_i^r\right)\exp\left(\beta\left(\phi_i^t\right)\right)}{\mathrm{BW}_{ref}\,4\pi d_i^2\,G_{Gmax}^r}, \tag{17}$$

where γ_i represents the contribution of each satellite to the EPFD formula (2). Large values of $\boldsymbol{\gamma}$ vector denote the satellites contributing mostly to EPFD. These are the critical satellites and their indexes, i_{crit}, are stored in the $\mathcal{I}_{crit}$ set. The intention is to only implement tilting for satellites in this set, and we would have $\theta_{i\neq i_{crit}} = 0$, accordingly. Now, we rewrite the problem formulation, applying the tilting method for the critical satellite set by changing the $L3$ constraint in (16) as,

$$\begin{aligned}
&\underset{q_i,\theta_i}{\text{minimize}} \left\| B\log_2\left(1+\frac{k_{i,u}\exp\left(q_i+\beta s_{i,u}\theta_i\right)}{v_u}\right)-D_u\right\|_2\\
&\text{s.t. } \tilde{L1} : 10\log_{10}\left(\sum_{i=1}^{N}\frac{AG_G^r(\phi_i^r)\exp\left(q_i+\beta(\phi_i^t+\theta_i)\right)}{\mathrm{BW}_{ref}\,4\pi d_i^2\,G_{Gmax}^r}\right)\\
&\qquad\qquad \leq \mathrm{EPFD_{thr}},\\
&L2 : q_i \leq \log(P_{\max}), \quad \forall i\\
&\tilde{L3} : 0 \leq \theta_{i_{crit}} \leq \theta_{\max}, \quad \forall i_{crit} \in \mathcal{I}_{crit}.
\end{aligned} \tag{18}$$

We observe that the objective function and the constraints are convex as elaborated in Section III-C, and accordingly the problem formulation is convex.

The procedure of our proposed solution is summarized in pseudo-code by Algorithm 1. First, the visible satellites to the GSO receiver are determined and the problem (18) is solved with zero tilting for all satellites to obtain the initial power allocations, p_i. Subsequently, the γ vector is calculated using (17), and if the condition $\frac{\gamma_i p_i}{10^{\mathrm{EPFD_{thr}}/10}} \geq \zeta_{thr}$ is satisfied, the satellite is identified as critical. Finally, the problem (18) is solved and the outputs are the optimized values for power transmission of the visible LEO satellite set and the optimized tilting angles of the critical satellites. The computational complexity of Algorithm 1 is concentrated in step 5 where the problem (18) is solved by the CVX [26]. The solution can be obtained by the standard interior-point method and we can assume the worst-case runtime to analyze the complexity. Following [27] and [28], the complexity of computation is calculated as $\mathcal{O}(\sqrt{N+M+1}(N+M)^3)$, where N is the number of visible satellites and M represents the number of critical satellites. It is worth noting that our proposed method, which restricts the tilting of satellites to critical ones, results in a reduced number of decision variables and decreased computational complexity.

Algorithm 1: Joint Power and Tilt Angle Optimization.

Input: System location information, system parameters, and EPFD limit.
Output: Visible satellite transmit powers, and critical satellite tilting angles.
1: Find visible satellites to the GSO receiver; index with $i \in \{1, 2, 3, .., N\}$,
2: Set zero tilting for all satellites, $\mathcal{I}_{crit} = \emptyset$, and solve (18),
3: Calculate γ_i from (17) for each satellite,
4: Find critical satellite set, $\mathcal{I}_{crit}$, for satellite indexes with $\frac{\gamma_i p_i}{10^{\mathrm{EPFD_{thr}}/10}} \geq \zeta_{thr}$,
5: Solve (18),
6: Calculate satellites power as $P_i^{opt} = exp(q_i^{opt})$,
7: **return** P_i^{opt}, $(\theta_{i_{crit}})^{opt}$

IV. SIMULATION RESULTS

In this section, we present the results of this study simulated in MATLAB. For the simulation setup, we have considered a Walker star NGSO satellite constellation at the altitude of 1200 km with 49 satellites in each of the 36 orbits, and a single GSO satellite. The single GSO ground station points its antenna in the direction of the latter. Different numbers of LEO users are considered in the simulations and their general characteristics along with satellite and GSO ground station details are given in Table 1. Note that the EPFD limit assumed for this study is based on the ITU RR, Article 22 [7]. We have considered the EPFD limit that should not be exceeded for zero percent of the time. As stated before, the LEO satellites are nadir-pointing and have a single beam. We have assumed the half-beamwidth antenna size equal to 13.9 degrees for LEO satellites. With this assumption, we are able to cover the earth's surface and ensure full geographical coverage and service.

In Fig. 3 we illustrate the visible satellites and their coverage for the GSO ground station where the GSO satellite has the same longitude and latitude as the GSO ground station. The geographical locations of NGSO satellites are marked by red plus markers and at this specific time, there are 47 of them visible to the ground station. The blue and black outlines depict the −3 and −5 dB beam contours, respectively. Furthermore, to assure our assumption of negligible interference towards the neighboring LEO satellites when applying tilting, we plotted Fig. 4. In this figure, we have assumed maximum tilting for the critical satellite and plotted the resulting -3 dB contour for both cases of tilting up or down. We can observe that in this worst scenario, the beam coverage contours do not cross the neighboring ones. Next, we present the EPFD evaluation and the performance of our proposed joint power and tilting technique.

TABLE 1. System Simulation Parameters

LEO constellation	
Altitude (Km)	1200
Orbit plane inclination	87.9°
Maximum transmit power	10 dBW
Maximum antenna gain	39.6 dBi
Downlink frequency	19.7 GHz
Bandwidth	200 MHz
Antenna pattern	[22]
Maximum tilt angle	10°
Approximated antenna gain coefficient, A	1.0632e+04
Approximated antenna gain coefficient, β	-0.0671
GSO satellite	
Altitude (Km)	35785.4
Longitude	30.6°
Latitude	0°
Downlink frequency	19.7 GHz
GSO ground station	
Minimium elevation angle	10°
Maximum receive gain	40.95 dBi
Noise temperature	240 K
Antenna pattern	[24]
LEO user ground station	
Maximum receive gain	40.95 dBi
Noise temperature	240 K
Antenna pattern	[24]
EPFD	
EPFD limit $(dB(W/m^2/1MHz))$	-173.4 [7]
Reference antenna diameter	70 cm

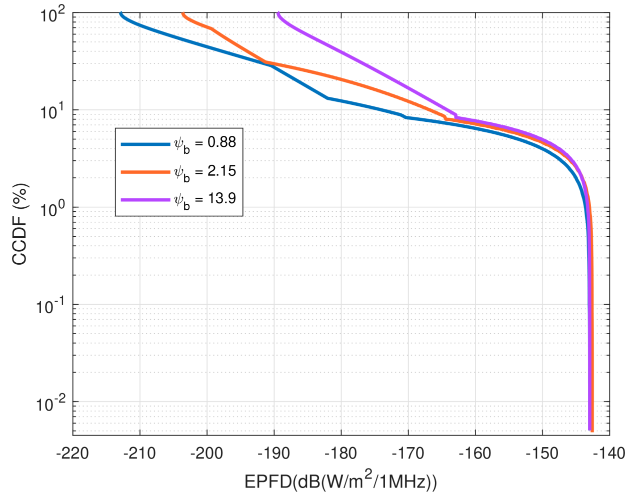

FIGURE 5. Distribution of EPFD probabilities in percent for downlink interference from LEO constellation at GSO ground station.

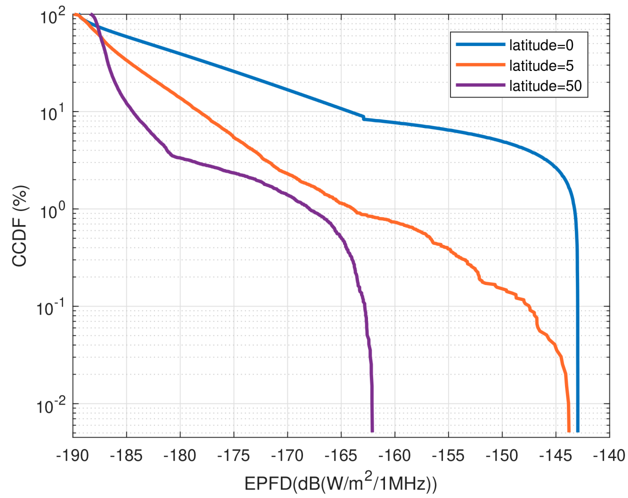

FIGURE 6. Distribution of EPFD probabilities in percent for downlink interference from LEO constellation at GSO ground station.

A. EPFD EVALUATION

As described in Section II-A, ITU evaluates the compliance of NGSO systems with regulations in terms of EPFD metric. The complementary cumulative distribution function (CCDF) of EPFD results is derived to evaluate the percentage of time in which EPFD has exceeded the radiated power limits. We evaluated the CCDF for our LEO constellation based on the procedure defined in [19]. The results are plotted in Fig. 5 for different transmit antenna half 3 dB beamwidth of the LEO satellites. Here we assumed co-located GSO and LEO earth stations on the equator with 30.6 degrees of longitude. Maximum transmission power is set to 10dBW for the LEO satellites. The plot indicates higher probabilities for the occurrence of larger EPFD levels as the transmitting antenna half 3 dB beamwidth increases and can be explained by higher power emissions for greater radiating beamwidth.

Furthermore, we evaluate the probability distribution of EPFD for different latitudes of the GSO ground station. Assuming an antenna beamwidth of 13.9 degrees for the LEO satellite, we plot the results in Fig. 6. As the latitude increases the inline events decrease and fewer probabilities for high emissions from LEO satellites are experienced. In fact, by moving the GSO earth station away from the equator, the antenna would align itself to point its main beam to the GSO satellite. As a result, this would lower the probabilities of inline events between station and the LEO satellites and also decrease the intensity of emissions due to the decreased receiving antenna gain and transmitting gain from LEO satellites. This is more evident for the plot with a latitude equal to 50 degrees where lower levels of EPFD are received and the probability for high EPFD levels has decreased.

In order to assess the EPFD levels received at the ground, we plot a snapshot of the EPFD from the LEO satellites in Fig. 7. We can see the EPFD variations given different positions of the GSO ground station receiver. The GSO satellite is assumed to be at longitude of 30.6 degrees East. The GSO ground station remains pointing at the GSO satellite, regardless of its position. The GSO satellite is represented by a star marker and the LEO satellites are shown by a plus marker in the figure. The EPFD values vary in the range of

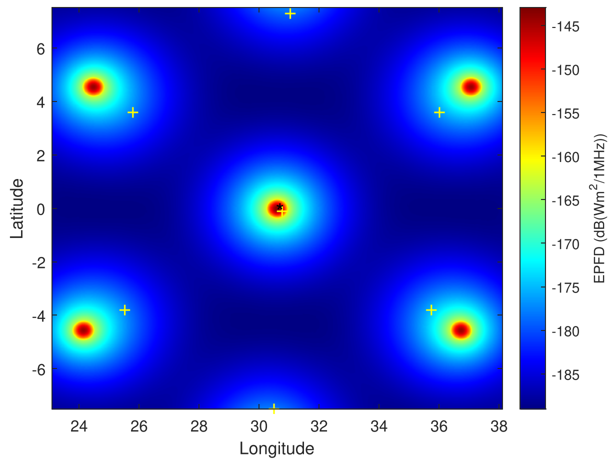

FIGURE 7. EPFD levels for different positions of the GSO ground station. GSO satellite position depicted with black star marker and LEO satellites with yellow plus markers.

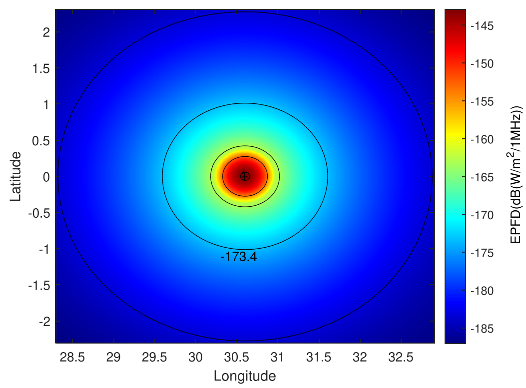

FIGURE 8. EPFD levels for different positions of the GSO ground station. Contours defining EPFD levels of −143.4, −153.4, −163.4, −173.4, and −183.4 dB(W/m^2/1 MHz).

approximately 50 dB. This is mainly caused by the narrow beamwidth of the highly directional GSO antenna receiver resulting in low receiving gains towards the LEO satellites. The highest EPFD levels occur when the GSO receiver, GSO satellite, and LEO satellite are in line which is in the middle of the figure. In this scenario, the LEO satellite pointing and the GSO earth station receiving directions are aligned. Also, for the other four neighboring satellites when the pointing direction of the GSO receiver is aligned to the LEO satellite, maximized receiving antenna gain and consequently high EPFD level is caused. This result should bring our attention to the fact that any in-line event would translate into high interference not only for the worst cases that LEO satellite passes over the GSO station.

In order to identify the critical satellites contributing the most to the total interfering power for a specific position, we present the previous results this time over a zoomed grid around the sub-satellite point of the GSO satellite location. Fig. 8 depicts EPFD contours to visualize the EPFD variation as a function of the receiver location, where the EPFD limit for

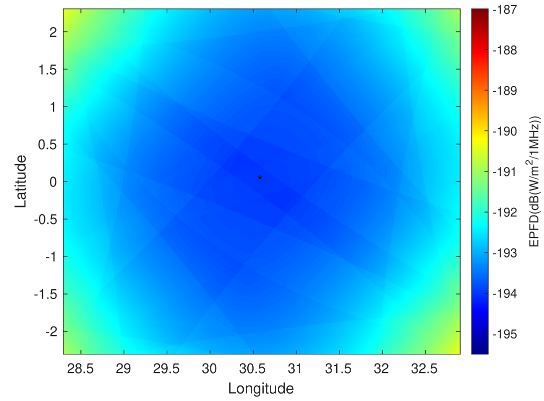

FIGURE 9. EPFD levels for different positions of the GSO ground station without critical satellite.

−173.4 dB(W/m^2/1 MHz) is outlined and the other contours define 10 dB differences. For comparison, Fig. 9 illustrates a scenario in which the closest LEO satellite has been switched off and it can be seen that for the sub-satellite point of the corresponding satellite, the EPFD results have decreased notably. This indicates that the neighboring satellites compared to the closest satellite in angular terms have less impact on the aggregate interfering power level. We can see the EPFD level is around −194 dB(W/m^2/1 MHz) for sub-point areas of the switched-off satellite which ensures ITU regulation compliance for those areas. We consider this fact in our optimization problem and employ it to approximate satellite selection for the tilt optimization procedure.

B. EVALUATION OF PROPOSED METHODS

We present results on the performance of our proposed solution for joint power and tilt angle optimization of LEO satellites. The demand satisfaction problem is solved for the LEO constellation and GSO receiver with the specifications given in Table 1. First, we compare the results for both cases of addressing the optimization problem, one involving solving the (16) and the other employing the (18). As elaborated in Section III-B we proposed (18) as a sub-optimal solution for the joint power and tilt angle optimization problem by considering a set of critical satellites and adapting the tilting strategy only for those specific satellites. To evaluate the performance under both optimal and sub-optimal solutions, we plotted the average demand satisfaction results for iterations over random positions of LEO users in Fig. 10. The GSO ground station is at 30.6 degrees of longitude at the equator and LEO satellites have 5 users. The observed differences between the two solutions can be characterized as negligible, indicating a minimal impact on the average demand satisfaction. We further investigate the performance and complexity of the two methods across different GSO locations. The comparison is presented in Table 2 where the GSO ground station is at 30.6 degrees of longitude and its latitude is varied from 0 to 0.4 degrees. The number of visible LEO satellites to the GSO ground station for these positions is equal to 47. As

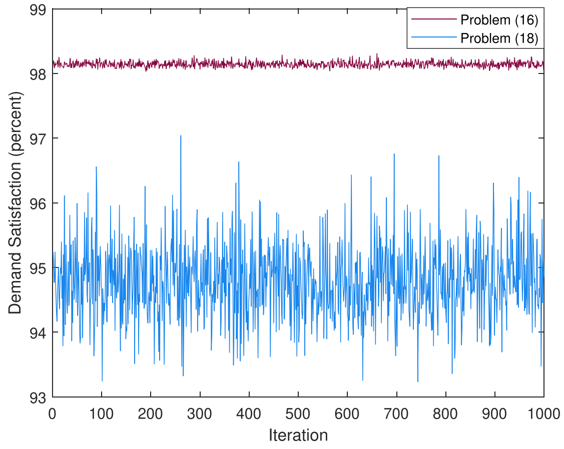

FIGURE 10. Average demand satisfaction percentage of visible satellites for iteration over random users' positions and satellite demand requests in the range of 4 and 6 Gbps.

TABLE 2. Comparison of Optimization Problem Results

	latitude = 0	latitude = 0.2	latitude = 0.4
Method	Number of tilted satellites		
Problem (16)	47	47	47
Problem (18)	1	1	1
Method	Decision variables		
Problem (16)	94	94	94
Problem (18)	48	48	48
Method	Average demand satisfaction of visible satellites		
Problem (16)	98.64%	98.98%	99.21%
Problem (18)	94.79%	95.24%	96.36%

we can see in the results, the solution of problem (16) tilts every visible LEO satellite while problem (18) only requires the tilting of a single satellite. This allows a significant reduction in the number of optimization variables, where the proposed heuristic method has approximately half the number of decision variables compared to the alternative approach. Consequently, the computational complexity is reduced by an order of magnitude in this scenario. This reduction simplifies the optimization process and contributes to a notable improvement in computational requirements. In contrast to the computational complexity differences, the two methods yield similar levels of demand satisfaction as evident from the table.

Based on the comparison, it can be concluded that the proposed approach using a critical satellite set yields results similar to those of the all-tilting method, with significantly less satellite tilting, resulting in savings on satellite energy consumption and management complexities. Therefore, for the remainder of the article, we will employ the problem (18) approach to obtain the joint power and tilt angle solution. For the scenarios presented here, based on our EPFD evaluations we set $\zeta_{thr} = 0.7$, which results in one single critical satellite.

TABLE 3. Demand Satisfaction (%) for Single User Scenario

GSO ground station	Optimization	Demand Satisfaction (%)	
		Critical Satellite	Other Satellites
latitude = 0	no Opt	0	100
	no EPFD	100	100
	Power	12.50	100
	Power + Tilt	32.28	100
latitude = 0.2	no Opt	0	100
	no EPFD	100	100
	Power	32.24	100
	Power + Tilt	47.86	100

In addition to the proposed technique, we consider benchmark schemes and derive the results for these four cases:

- ”no Opt”: there is no optimization applied for the transmission power, and the satellite beam either transmits with the maximum power or terminates the transmission. If the EPFD limit is exceeded, the critical satellite is switched off.
- ”no EPFD”: we assume there is no EPFD limit so we relax the $\tilde{L}1$ constraint and also assume no tilting for the satellites. This case presents the possible demand satisfaction when no interference restrictions are applied.
- ”Power”: we solve the problem by solely focusing on power optimization under the EPFD constraint.
- ”Power+Tilt”: we adopt our proposed solution, the joint power and tilt angle optimization method in the problem (18).

First, we assume a single LEO user per beam with a random position. The demand for the user is a random value in the range of minimum 0.8 Gbps and a maximum of 1.2 Gbps. The user's location and demand randomly change for each iteration. Table 3 shows the results of the single-user scenario, where the demand satisfaction presented in percent is calculated as the ratio of capacity allocated to each user divided by the demanded capacity request. Here, results are presented for the GSO ground station in 30.6 degrees of longitude and for two latitudes of 0 and 0.2 degrees. As we can see in the “no Opt” results for both latitudes, the EPFD limit is surpassed for the critical satellite, and in order to comply with the interference regulations the satellite should interrupt its transmission. However, by applying power optimization we are able to increase demand satisfaction. Adding the tilting and applying the proposed joint optimization solution, further rises the demand satisfaction. In particular, we can see the benefit of the method for the 0.2-degree latitude case where the demand satisfaction of the critical satellite has improved by more than 47%. It is worth noticing that the strict EPFD limits are impacting the LEO service since complete user demand satisfaction cannot be achieved for the critical satellite.

Next, we present the results for 5 LEO users randomly positioned at the service area of each LEO satellite. Due to the single beam per satellite assumption, in the multi-user

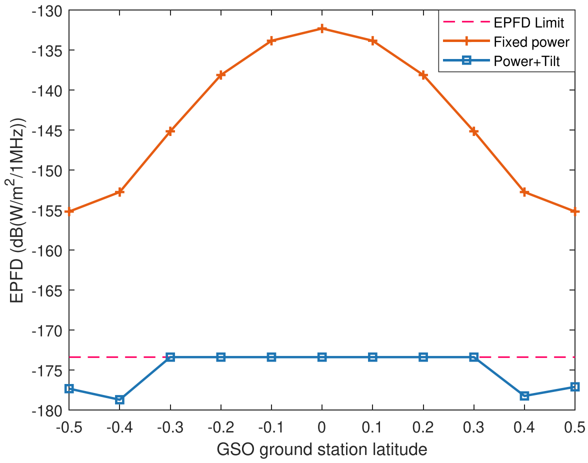

FIGURE 11. Resulting EPFD for different GSO ground station latitudes. Five users per satellite and random satellite demand requests in the range of 4 and 6 Gbps.

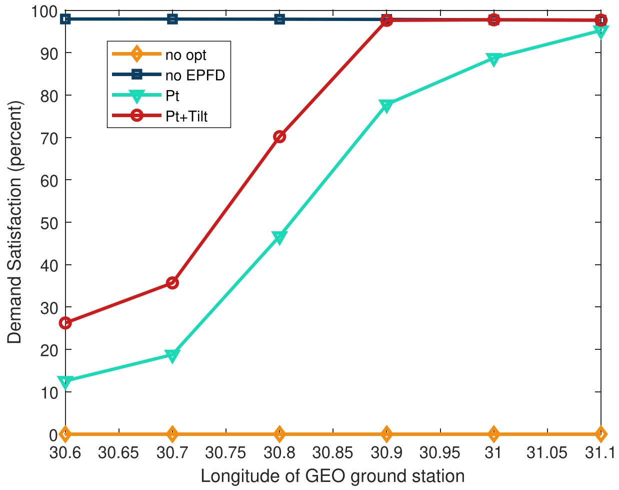

FIGURE 12. Demand satisfaction percentage of the critical satellite for different GSO ground station longitudes. Five users per satellite and random satellite demand requests in the range of 4 and 6 Gbps.

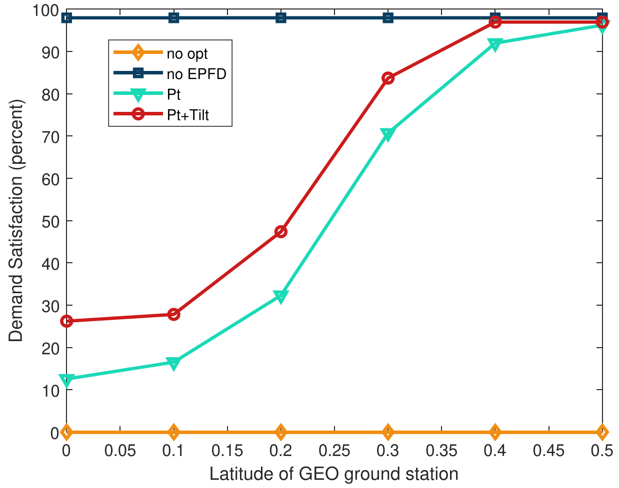

FIGURE 13. Demand satisfaction percentage of the critical satellite for different GSO ground station latitudes. Five users per satellite and random satellite demand requests in the range of 4 and 6 Gbps.

scenario, it is necessary to optimize the satellite's power considering all users and minimize the differences in the allocated capacity to users and their demanded requests. It is assumed that the aggregated satellite demand request is randomly distributed in the range of [4, 6] Gbps and the users have the same demand request equally divided among them.

Prior to presenting demand satisfaction results, we evaluate the resulting EPFD levels at the GSO ground station with our proposed interference mitigation method and a fixed power scenario where the satellite employs no mitigation techniques and transmits at a maximum power level. Fig. 11 demonstrates the results where the ground station is at 30.6 degrees of longitude and its latitude changes from -0.5 to 0.5 degrees. In contrast to the fixed power case, which consistently exceeds the allowed EPFD limit for different positions, our method ensures that the EPFD remains within the specified limit. This performance highlights the effectiveness of our approach in mitigating interference, even in severe scenarios, thus ensuring robust interference control. The demand satisfaction results of this scenario are plotted for different placements of GSO ground stations in longitude and latitude grids. First, Fig. 12 presents results where the GSO station is on the equator and its longitude changes from 30.6 degrees which is the GSO satellite's longitude, to 31.1 degrees. We observe that in these positions the critical satellite should be switched off. Whereas, by applying power and tilt optimization we can improve demand satisfaction. Next, we fix the longitude to 30.6 degrees and increase the latitude, see Fig. 13. The satisfaction enhancement through power and tilt optimization is evident in this scenario as well. For a few degrees from the GSO station, we can achieve 100% of user demand satisfaction and comply with the interference regulations, contrary to the zero service availability when applying no interference mitigation technique. By applying our proposed method the NGSO constellation is able to maintain user service instead of switching off for the high EPFD events.

Finally, we apply our method for a period of time where the LEO satellite passes over a single GSO earth station. The simulation results are illustrated in Fig. 14 considering 5 users per LEO satellite. The GSO ground station and users positions are presented for this scenario and the LEO satellite positions for the first snapshot and final simulation time are illustrated in Fig. 14(a) and (b), respectively. It should be noted that only the satellites in the field of view of the GSO ground station are shown based on our optimization algorithm. The EPFD level on the GSO station is measured for each time step and is compared with the limit. In Fig. 14(c) for latitudes close to the GSO ground station, the EPFD limit is not satisfied when applying fixed power transmission at LEO satellites. We adopt our joint power and tilt management method and

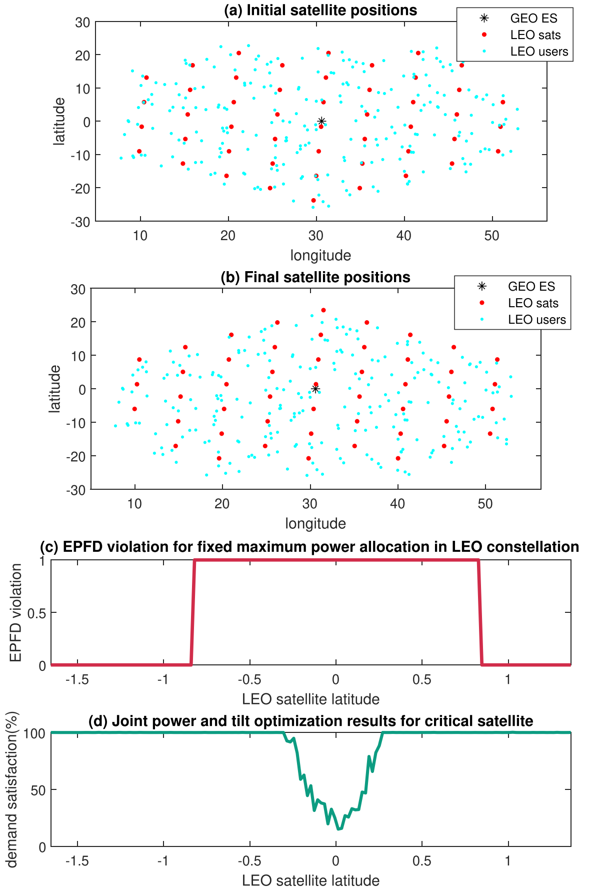

FIGURE 14. Passing of LEO satellite over GSO ground station.

derive the demand satisfaction results for the critical satellite in Fig. 14(d). Except for the positions where the LEO satellite is right above the GSO station, the users' demands are met. On the contrary, the fixed power allocation would require the critical satellite to be turned off for the whole EPFD violation period. this translates into service interruption for the satellite users in this period which comprises a large part of the satellite visibility and a notable area of the coverage.

V. CONCLUSION

The prevalence of mega-constellation NGSO satellites evokes concerns about aggravated damages to the primary co-existing GSO systems. We have presented a joint transmit power control and tilt angle optimization approach, which minimizes the difference between the traffic demand and offered capacity of the LEO constellation under ITU regulatory interference constraints. Simulation results reveal the efficiency of the proposed solution for interference mitigation and user demand satisfaction especially, in scenarios where the direction of arrival for signals coming from LEO and GSO satellites coincide at the ground station. Thus, our work opens the door to a more systematic regulation-aware design of satellite payloads and resource allocation techniques for future LEO satellite mega-constellations.

REFERENCES

[1] M. Giordani and M. Zorzi, "Non-terrestrial networks in the 6G era: Challenges and opportunities," *IEEE Netw.*, vol. 35, no. 2, pp. 244–251, Mar./Apr. 2021.

[2] X. Lin, S. Cioni, G. Charbit, N. Chuberre, S. Hellsten, and J.-F. Boutillon, "On the path to 6G: Embracing the next wave of low Earth orbit satellite access," *IEEE Commun. Mag.*, vol. 59, no. 12, pp. 36–42, Dec. 2021.

[3] S. K. Sharma et al., Satellite Communications in the 5G Era, (Telecommunications Series): Inst. Eng. Technol., 2018. [Online]. Available: https://digital-library.theiet.org/content/books/te/pbte079e

[4] X. Zhu and C. Jiang, "Integrated satellite-terrestrial networks toward 6G: Architectures, applications, and challenges," *IEEE Internet Things J.*, vol. 9, no. 1, pp. 437–461, Jan. 2022.

[5] O. B. Osoro and E. J. Oughton, "A techno-economic framework for satellite networks applied to low Earth orbit constellations: Assessing Starlink, OneWeb and Kuiper," *IEEE Access*, vol. 9, pp. 141611–141625, 2021.

[6] H. Al-Hraishawi, H. Chougrani, S. Kisseleff, E. Lagunas, and S. Chatzinotas, "A survey on non-geostationary satellite systems: The communication perspective," *IEEE Commun. Surv. Tut.*, vol. 25, no. 1, pp. 101–132, Firstquarter 2022.

[7] ITU-R, "Radio regulations," ITU-R, Geneva, Switzerland, 2020.

[8] B. A. Homssi et al., "Next generation mega satellite networks: Opportunities, challenges, and performance," 2021. [Online]. Available: https://arxiv.org/abs/2110.04231

[9] A. Hills, J. M. Peha, and J. Munk, "Feasibility of using beam steering to mitigate Ku-band LEO-to-GEO interference," *IEEE Access*, vol. 10, pp. 74023–74032, 2022.

[10] F. Öztürk and A. Kara, "Exclusion zone minimization and optimal operational mode selection for co-existent geostationary and non-geostationary satellites," *Int. J. Satell. Commun. Netw.*, vol. 40, no. 3, pp. 191–203, 2022. [Online]. Available: https://onlinelibrary.wiley.com/doi/abs/10.1002/sat.1433

[11] C. Braun, A. M. Voicu, L. Simić, and P. Mähönen, "Should we worry about interference in emerging dense NGSO satellite constellations?," in *Proc. IEEE Int. Symp. Dyn. Spectr. Access Netw.*, 2019, pp. 1–10.

[12] M. Jalali, F. Ortiz-Gomez, F. Lagunas, S. Kisseleff, L. Emiliani, and S. Chatzinotas, "Radio regulation compliance of NGSO constellations' interference towards GSO ground stations," in *Proc. IEEE Int. Symp. Pers. Indoor Mobile Radio Commun.*, 2022, pp. 1425–1430.

[13] P. Gu, R. Li, C. Hua, and R. Tafazolli, "Dynamic cooperative spectrum sharing in a multi-beam LEO-GEO co-existing satellite system," *IEEE Trans. Wireless Commun.*, vol. 21, no. 2, pp. 1170–1182, Feb. 2022.

[14] W. U. Khan, Z. Ali, E. Lagunas, S. Chatzinotas, and B. Ottersten, "Rate splitting multiple access for cognitive radio GEO-LEO co-existing satellite networks," 2022. [Online]. Available: https://arxiv.org/abs/2208.02924

[15] C. Wang, D. Bian, S. Shi, J. Xu, and G. Zhang, "A novel cognitive satellite network with GEO and LEO broadband systems in the downlink case," *IEEE Access*, vol. 6, pp. 25987–26000, 2018.

[16] OneWeb, "OneWeb non-geostationary satellite system (LEO) phase 1: Modification to authorized system," OneWeb, London, U.K. [Online]. Available: https://fcc.report/IBFS/SAT-MPL-20200526-00062/2379565.pdf

[17] T. Li, J. Jin, W. Li, Z. Ren, and L. Kuang, "Research on interference avoidance effect of OneWeb satellite constellation's progressive pitch strategy," *Int. J. Satell. Commun. Netw.*, vol. 39, no. 5, pp. 524–538, 2021. [Online]. Available: https://onlinelibrary.wiley.com/doi/abs/10.1002/sat.1399

[18] C. Zou, H. Wang, J. Chang, F. Shao, L. Shang, and G. Li, "Optimal progressive pitch for OneWeb constellation with seamless coverage," *Sensors*, vol. 22, no. 16, 2022, Art. no. 6302. [Online]. Available: https://www.mdpi.com/1424-8220/22/16/6302

[19] ITU-R, "Functional description to be used in developing software tools for determining conformity of non-geostationary-satellite orbit fixed satellite service systems or networks with limits contained in article 22 of the radio regulations," Tech. Rep. S.1503-3, 2018.

[20] 3GPP, "Study on new radio (NR) to support non-terrestrial networks," 3GPP, Marseille, France, Tech. Rep. 38.811, 2019.

[21] ITU-R, "Attenuation by atmospheric gases and related effects," *ITU-R, Geneva, Switzerland, Tech. Rep. P.676-13*, 2022.

[22] International Telecommunication Union Radiocommunication Sector, "Satellite antenna radiation patterns for non-geostationary orbit satellite antennas operating in the fixed-satellite service below 30 GHz," *ITU-R, Geneva, Switzerland, Tech. Rep. S.1528*, 2001.

[23] ITU-R, "Satellite antenna radiation pattern for use as a design objective in the fixed-satellite service employing geostationary satellites," *ITU-R, Geneva, Switzerland, Rep. Tech. S.672-4*, 1997.

[24] ITU-R, "Reference FSS Earth-station radiation patterns for use in interference assessment involving non-GSO satellites in frequency bands between 10.7 GHz and 30 GHz," *ITU-R, Geneva, Switzerland, Tech. Rep. S.1428-1*, 2001.

[25] S. Boyd and L. Vandenberghe, *Convex Optimization*. New York, NY, USA: Cambridge Univ. Press, 2004.

[26] M. Grant and S. Boyd, "CVX: Matlab software for disciplined convex programming, version 2.1," 2014. [Online]. Available: http://cvxr.com/cvx

[27] A. Ben-Tal and A. S. Nemirovskiaei, "Lectures on modern convex optimization: Analysis," *Algorithms Eng. Appl. USA: Soc. Ind. Appl. Math.*, 2001.

[28] M. T. Kabir, M. R. A. Khandaker, and C. Masouros, "Interference exploitation in full-duplex communications: Trading interference power for both uplink and downlink power savings," *IEEE Trans. Wireless Commun.*, vol. 17, no. 12, pp. 8314–8329, Dec. 2018.

MAHDIS JALALI (Graduate Student Member, IEEE) received the B.Sc. and M.Sc. degrees from the Department of Electrical Engineering, Amirkabir University of Technology (Tehran Polytechnic), Tehran, Iran. She is currently working toward the Ph.D. degree with SIGCOM Group, SnT, University of Luxembourg. Her research interests include satellite communication, resource management, and machine learning approaches for wireless communication systems.

FLOR ORTIZ (Member, IEEE) received the B.S. degree in telecommunications engineering and the M.S. degree in electrical engineering-telecommunications from the Universidad Nacional Autónoma de México, Mexico City, Mexico, in 2015 and 2016, respectively, and the Ph.D. degree in telecommunication engineering from the Universidad Politecnica de Madrid (UPM), Madrid, Spain, in 2021. During the Ph.D., she performed a research period with the University of Bologna, Bologna, Italy. She started a close collaboration between the UPM and University of Bologna, opening a new research line for both groups on applying Machine Learning for radio resource management. She is a Research Associate with the Interdisciplinary Centre for Security, Reliability, and Trust, University of Luxembourg. Her research interests include implementing cutting-edge machine learning techniques including continual learning and and neuromorphic computing for operations in satellite communications systems.

EVA LAGUNAS (Senior Member, IEEE) received the M.Sc. and Ph.D. degrees in telecommunications engineering from the Polytechnic University of Catalonia, Barcelona, Spain, in 2010 and 2014, respectively. From 2009 to 2013, she was a Research Assistant with the Department of Signal Theory and Communications, UPC. During the summer of 2009, she was a Guest Research Assistant with the Department of Information Engineering, Pisa, Italy. From November 2011 to May 2012, she held a visiting research appointment with the Center for Advanced Communications, Villanova University, Villanova, PA, USA. In 2014, she joined the Interdisciplinary Centre for Security, Reliability and Trust (SnT), University of Luxembourg, where she is currently a Research Scientist. Her research interests include terrestrial and satellite system optimization, spectrum sharing, resource management, and machine learning.

STEVEN KISSELEFF (Senior Member, IEEE) received the M.Sc. degree in information technology from the Technical University of Kaiserslautern, Kaiserslautern, Germany, in 2011 and the Ph.D. degree in electrical engineering from the Friedrich-Alexander University of Erlangen-Nürnberg (FAU), Erlangen, Germany, in 2017. In 2018, he joined the SIGCOM Research Group, SnT, University of Luxembourg, where he is currently a Research Scientist. His research interests include design and optimization of satellite networks, multi-antenna systems, receiver synchronization, and Internet of Things.

LUIS EMILIANI (Senior Member, IEEE) received the B.E.E. and M.Eng. degree from Universidad Pontificia Bolivariana, Medellin, Colombia, in 1999 and 2003, respectively. He is with SES S.A., Betzdorf, Luxembourg, in the Fleet Advancement Group responsible for setting and developing SES's communications satellite fleet strategy and leading the fleet planning process. His research interest focuses on the application of propagation techniques to solve practical sharing and system design scenarios. Mr. Emiliani is a Chartered Engineer (C.Eng.) with the U.K. Engineering council and Member of the Institution of Engineering and Technology.

SYMEON CHATZINOTAS (Fellow, IEEE) received the M.Eng. degree in telecommunications from the Aristotle University of Thessaloniki, Thessaloniki, Greece, in 2003 and the M.Sc. and Ph.D. degrees in electronic engineering from the University of Surrey, Guildford, U.K., in 2006 and 2009 respectively. He is currently Full Professor/Chief Scientist I and the Head of the Research Group SIGCOM, Interdisciplinary Centre for Security, Reliability and Trust, University of Luxembourg. He is also an Adjunct Professor with the Department of Electronic Systems, Norwegian University of Science and Technology, Trondheim, Norway, and a Collaborating Scholar of the Institute of Informatics & Telecommunications, National Center for Scientific Research, Demokritos. In the past, he has lectured as Visiting Professor at the University of Parma, Parma, Italy, and contributed in numerous R&D projects for the Institute of Telematics and Informatics, Center of Research and Technology Hellas and Mobile Communications Research Group, Center of Communication Systems Research, University of Surrey. He has authored more than 700 technical papers in refereed international journals, conferences and scientific books and has received numerous awards and recognitions, including the IEEE Fellowship and an IEEE Distinguished Contributions Award. He is with the Editorial Board of IEEE TRANSACTIONS ON COMMUNICATIONS, IEEE OPEN JOURNAL OF VEHICULAR TECHNOLOGY and *International Journal of Satellite Communications and Networking*.